PLOS ONE

RESEARCH ARTICLE

# Identification of putative Type-I sex pheromone biosynthesis-related genes expressed in the female pheromone gland of *Streltzoviella insularis*

**Yuchao Yang, Jing Tao*, Shixiang Zong***

Beijing Key Laboratory for Forest Pest Control, School of Forestry, Beijing Forestry University, Beijing, China

* taojing1029@hotmail.com (JT); zongsx@126.com (SXZ)

Check for updates

OPEN ACCESS

**Citation:** Yang Y, Tao J, Zong S (2020) Identification of putative Type-I sex pheromone biosynthesis-related genes expressed in the female pheromone gland of *Streltzoviella insularis*. PLoS ONE 15(1): e0227666. https://doi.org/10.1371/journal.pone.0227666

**Editor:** J. Joe Hull, USDA Agricultural Research Service, UNITED STATES

**Received:** August 5, 2019

**Accepted:** December 24, 2019

**Published:** January 16, 2020

**Copyright:** © 2020 Yang et al. This is an open access article distributed under the terms of the Creative Commons Attribution License, which permits unrestricted use, distribution, and reproduction in any medium, provided the original author and source are credited.

**Data Availability Statement:** All raw reads files are available from the NCBI SRA database (accession number SRP179142).

**Funding:** This research was funded by Fundamental Research Funds for the Central Universities (2018ZY24) and Beijing's Science and Technology Planning Project (Z171100001417005). The funders had no role in study design, data collection and analysis, decision to publish, or preparation of the manuscript.

## Abstract

Species-specific sex pheromones play key roles in moth sexual communication. Although the general pathway of Type-I sex pheromone biosynthesis is well established, only a handful of genes encoding enzymes involved in this pathway have been characterized. *Streltzoviella insularis* is a destructive wood-boring pest of many street trees in China, and the female sex pheromone of this species comprises a blend of (*Z*)-3-tetradecenyl acetate, (*E*)-3-tetradecenyl acetate, and (*Z*)-5-dodecenyl acetate. This organism therefore provides an excellent model for research on the diversity of genes and molecular mechanisms involved in pheromone production. Herein, we assembled the pheromone gland transcriptome of *S. insularis* by next-generation sequencing and identified 74 genes encoding candidate key enzymes involved in the fatty acid biosynthesis, β-oxidation, and functional group modification. In addition, tissue expression patterns further showed that an acetyl-CoA carboxylase and two desaturases were highly expressed in the pheromone glands compared with the other tissues, indicating possible roles in *S. insularis* sex pheromone biosynthesis. Finally, we proposed putative *S. insularis* biosynthetic pathways for sex pheromone components and highlighted candidate genes. Our findings lay a solid foundation for understanding the molecular mechanisms underpinning *S. insularis* sex pheromone biosynthesis, and provide potential targets for disrupting chemical communication that could assist the development of novel pest control methods.

## Introduction

Lepidoptera sex pheromones, which are usually secreted by female moths to attract conspecific males, play a key role in sexual communication, and are used as a monitoring and trapping tool in integrated pest management programs [1–3]. In general, moth sex pheromones are composed of two or more components in a unique ratio, and are classified into four types (Type-I, Type-II, Type-III, and Type-0) according to their site of production, chemical structure, and biosynthetic features [4]. Type-I sex pheromones are alcohols and their derivatives

**Competing interests:** The authors have declared that no competing interests exist.

(acetates and aldehydes) with long straight chains ($C_{10}$–$C_{18}$) which are used by most moths [1, 5]. Type-II sex pheromones are composed of $C_{17}$–$C_{23}$ hydrocarbons with two or three double bonds at the three, six, or nine positions, or their corresponding epoxide derivatives [1, 5]. Compared with Type-I and Type-II sex pheromones, Type-III sex pheromones with one or more methyl branches possess distinct biosynthetic features, and these components include $C_{17}$–$C_{23}$ saturated and unsaturated hydrocarbons, as well as functionalized hydrocarbons [5]. Type-0 sex pheromones, short-chain secondary alcohols or ketones similar to some general plant volatile compounds, are utilized by the oldest non-ditrysian lineages of Lepidoptera species and are thought to represent the ancestral type of sex pheromone [5–7]. Moth sex pheromones, particularly Type-I, are mainly biosynthesized in and released from the sex pheromone gland (PG) located at the inter-segmental membrane between the eighth and ninth abdominal segments [4, 8].

The general biosynthesis pathway for Type-I sex pheromones in moths is well established; they are synthesized *de novo* through modified fatty acid biosynthesis pathways, and several enzymatic reactions are indispensable, including desaturation, oxidation, reduction, and acetylation [1, 4, 9–12]. All carbon atoms of the fatty acid are derived from acetyl-CoA, acetyl-CoA carboxylase (ACC) converts acetyl-CoA into the fatty acid precursor malonyl-CoA [13], and fatty acid synthetase (FAS) produces palmitic acid (C16) or stearic acid (C18) using acetyl-CoA and malonyl-CoA as substrate and NADPH as reducing agent [14–15]. Double bonds are introduced into the acyl chain at specific positions by desaturases (DESs), of which seven (Δ5 [16], Δ6 [17], Δ9 [18], Δ10 [19], Δ11 [20], Δ12 [11], and Δ14 [21]) have been identified in Lepidoptera species based on signature motifs. For instance, Δ9-desaturases have been divided into two groups: one with a substrate chain length preference of C16 >C18 (NPVE motif), and the other with a substrate chain length preference of C18 >C16 (KPSE motif) [22]. Subsequently, the unsaturated fatty acid is subjected to chain-shortening by β-oxidation, generating sex pheromone precursors of specific chain length [23], and the carbonyl carbon is modified to form an oxygenated functional group, such as an aldehyde, alcohol, or acetate ester, and these modifications involve some key biosynthesis enzymes; fatty acyl-CoA reductase (FAR) converts these acyl chains into fatty alcohols that act as actual sex pheromone components in various moths [24–26], but most fatty alcohols are either oxidized into the corresponding aldehyde by dehydrogenases [27–28] or esterified to form acetate esters by acetyltransferase (ATF) [29–31], resulting in the final functional groups.

*Streltzoviella insularis* (Staudinger) (Lepidoptera: Cossidae) is a destructive wood-boring pest and occurs in many provinces and cities in China. It mainly damages various street trees, such as *Fraxinus americana*, *Ginkgo biloba*, *Sophora* spp., and *Ulmus* spp., causing great economic losses to urban forestry [32–34]. The female sex pheromone of *S. insularis* is a blend of (*Z*)-3-tetradecenyl acetate (Z3-14:OAc), (*E*)-3-tetradecenyl acetate (E3-14:OAc), and (*Z*)-5-dodecenyl acetate (Z5-12:OAc) [35–36], and these acetate esters are typical of Type-I sex pheromones. These different components indicate the involvement of different desaturases, β-oxidases, and reductases during sex pheromone production. Characterization of the genes encoding putative key enzymes involved in this process may not only help to elucidate the sex pheromone biosynthesis pathway in *S. insularis*, but may also provide potential targets for disrupting sexual communication for pest control purposes. Hence, in the present study, we first constructed a transcriptome library of *S. insularis* PGs and identified a series of genes that might be involved in sex pheromone biosynthesis. Tissue expression patterns and phylogenetic analysis were performed to postulate the potential functions of the identified genes. Based on the results, we propose putative biosynthetic pathways for the sex pheromone components in *S. insularis*.

## Materials and methods

### Ethics statement

*S. insularis* is not on the List of Endangered and Protected Animals in China. The Beijing Municipal Bureau of Landscape and Forestry issued a permit for field collection.

### Sample collection

*S. insularis* individuals were collected from *Fraxinus americana* at Beijing Forestry University North Road, Haidian District, Beijing, China, in May 2017. Damaged trunks were chopped down, taken to the laboratory, and larvae inside trunks were fed on the phloem and xylem of the host under natural environmental conditions. Adult moths were sexed after emergence according to the genitalia. The pheromone gland and associated ovipositor valves, as well as parts of the terminal abdominal segments (together abbreviated as PG) were dissected from 1-day-old and 2-day-old female adults during the scotophase, which is reported to be the calling period of this moth [35, 37]. In addition, antennae and legs were also collected at the same time, immediately placed in RNAlater (Ambion, Austin, TX, USA), and stored at -80˚C.

### RNA extraction

Total RNA was extracted from 15 PGs (seven PGs from 1-day-old females and eight PGs from 2-day-old females) using TRIzol reagent (Invitrogen, Carlsbad, CA, USA) following the manufacturer's instructions, with three biological replicates. RNA purity was evaluated with a NanoDrop 2000 instrument (Thermo, Waltham, MA, USA), and RNA concentration was measured using a Qubit RNA Assay Kit and a Qubit 2.0 Fluorimeter (Life Technologies, CA, USA). RNA integrity was determined by an Agilent Bioanalyzer 2100 system (Agilent Technologies, CA, USA), and RNA degradation and contamination were monitored by 1% agarose gels to ensure the quality of the RNA samples for subsequent transcriptome sequencing.

### cDNA library construction and Illumina sequencing

cDNA library construction and Illumina sequencing of samples were performed at Shanghai Majorbio Bio-pharm Technology Co., Ltd. (Shanghai, China). According to the TruSeq RNA Sample Preparation Guide V2 (Illumina), mRNA was purified from total RNA using Oligo (dT) magnetic beads, then fragmented by adding fragmentation buffer. Random hexamer primers were used to synthesize first-strand cDNA, followed by synthesis of the second strand using dNTPs, RNaseH, and DNA polymerase I. All remaining overhangs were converted into blunt ends via polymerase. After end-repair, poly-A tailing, and ligation of adapters, 150–200 bp cDNA fragments were purified using an AMPure XP system (Beckman Coulter, Beverly, MA, USA), and 3μl USER Enzyme (NEB, USA) was incubated with size-selected, adaptor-ligated cDNA at 37˚C for 15 min followed by incubation at 95˚C for 5 min, prior to PCR amplification. PCR products were purified using an AMPure XP system, and library quality was assessed on the Agilent Bioanalyzer 2100 system. Finally, *S. insularis* cDNA libraries were sequenced on an Illumina Hiseq 4000 platform, and paired-end reads were generated.

### Sequence assembly and functional annotation

To obtain the clean reads, the raw reads were processed to remove low-quality reads and adapter sequences. Then, GC Content, Q20 and Q30 were used to assess the sequencing quality. The qualified reads assembly was carried out with the short reads assembling program-Trinity [38]. The largest alternative splicing variants in the Trinity results were called unigenes. The annotation of unigenes was performed by the National Center for Biotechnology

Information (NCBI) BLASTx searches against the non-redundant (Nr) protein database, with a cut-off E-value of $10^{-5}$. Unigenes were also annotated using other protein databases including Gene Ontology (GO) [39], Clusters of Orthologous Groups of proteins (COG) [40], and Kyoto Encyclopedia of Genes and Genomes (KEGG) [41]. The longest open reading frame (ORF) for each unigene was determined by the NCBI ORF Finder tool (http://www.ncbi.nlm.nih.gov/gorf/gorf.html). Fragments per kilobase of exon per million mapped reads (FPKM) values were calculated by RSEM (RNA-Seq by Expectation-Maximization) with default parameters represented gene expression in *S. insularis* PG tissue [42].

## Identification of putative genes involved in sex pheromone biosynthesis

Putative unigenes involved in sex pheromone biosynthesis of *S. insularis* were confirmed by analysis with the BLASTx program. All candidate pheromone biosynthesis-activating neuropeptide receptor (PBANR), acetyl-CoA carboxylase (ACC), fatty acid synthase (FAS), desaturase (DES), acyl-CoA oxidase (ACO), acyl-CoA dehydrogenase (ACD), enoyl-CoA hydratase (ECH), L-3-hydroxyacyl-CoA dehydrogenase (HCD), 3-ketoacyl-CoA thiolase (KAT), fatty acyl-CoA reductase (FAR), alcohol dehydrogenase (AD), aldehyde reductase (AR) and acetyltransferase (ATF) genes were manually checked by tBLASTn in NCBI online.

## Sequence and phylogenetic analyses

Amino acid sequences of candidate desaturases were aligned with those of other insect species using ClustalW by MEGA (Version 5.0) [43]. Phylogenetic tree construction was performed using the neighbor-joining method as implemented in MEGA (Version 5.0) with a *p*-distance model and pairwise deletion of gaps. Bootstrap support of tree branches was assessed by resampling amino acid positions 1000 times [44]. Phylogenetic trees were colored and arranged using FigTree (Version 1.4.2) [45].

## Expression analysis by quantitative real-time PCR (RT-qPCR)

Expression patterns of putative ACC and DES genes in different tissues (antennae, legs, and PGs) were analyzed by RT-qPCR using a Bio-Rad CFX96 PCR System (Hercules, CA, USA). Total RNA was extracted from 25 antennae, 10 legs, and 15 PGs of female moths following the method described above, and transcribed into cDNA using a PrimeScript RT Reagent Kit with gDNA Eraser (No. RR047A; TaKaRa, Shiga, Japan). Gene-specific primers were designed using Primer 3 Plus (http://www.bioinformatics.nl/cgi-bin/primer3plus/primer3plus.cgi) and are listed in S1 Table. The *S. insularis* actin gene served as an internal reference gene. Each RT-qPCR mixture was composed of 12.5 μl of TB Green Premix Ex Taq II (Tli RNaseH Plus; No. RR820A; TaKaRa), 1 μl of forward primer (10 μM), 1 μl of reverse primer (10 μM), 2 μl of cDNA, and 8.5 μl of sterilized $H_2O$. RT-qPCR cycling parameters were as follows: 95˚C for 30 s, followed by 40 cycles at 95˚C for 5 s and 60˚C for 30 s, and 65˚C to 95˚C in increments of 0.5˚C for 5 s to generate melting curves. To check reproducibility, each reaction for each tissue was performed with three biological replicates and three technical replicates. Negative controls without template were included in each experiment. Relative expression levels were calculated according to the comparative $2^{-\Delta\Delta Ct}$ method (the amplification efficiency was close to 100% for 12 genes) [46]. Leg samples were used for calibration, and actin was used for calculating and normalizing target gene expression, and correcting for sample to sample variation. Data in the form of means ± standard error (SE) from different samples were subjected to one-way nested analysis of variance, followed by Tukey's honestly significant difference tests, implemented in SPSS Statistics 22.0 (IBM, Chicago, IL, USA).

## Results and discussion

### Illumina sequencing and unigene assembly

We constructed cDNA libraries utilizing mRNAs from *S. insularis* PG tissue samples as template with an Illumina Hiseq 4000 platform, and included three biological replicates. A total of 63,881,910, 54,395,274, and 58,219,720 raw reads were obtained from each library. After removing low-quality reads and adaptors, we finally acquired 60,708,992, 51,561,536, and 55,208,486 clean reads, respectively (Table 1). Subsequently, assembly of all clean reads together resulted in 30,307 unigenes with an N50 value of 2072 bp, an average length of 1385 bp, and a longest length of 26,771 bp. Raw reads have been deposited in the NCBI SRA database under accession number SRP179142.

### Homology searching and functional annotation

Among the 30,307 unigenes, 16,304 (53.80%) were successfully matched using the BLASTx homology search (cut-off E-value of $10^{-5}$) to entries in the NCBI Nr protein database. The best matches were obtained for *Danaus plexippus* sequences (30.62%), followed by *Bombyx mori* (25.94%), *Papilio xuthus* (2.54%), and *Acyrthosiphon pisum* (1.63%), as shown in Fig 1.

GO annotation was used to classify the unigenes into three functional groups (molecular function, cellular component, and biological process) according to the GO categories. Of 30,307 unigenes identified in *S. insularis*, 8053 (26.57%) were annotated. As shown in Fig 2, 20,072 unigenes were assigned to the 'molecular function' category, and 'binding' (4141 unigenes, 43.14%) and 'catalytic activity' (3695 unigenes, 38.49%) were the most highly represented terms in this category. A total of 12,115 unigenes were assigned to GO terms in the 'cellular component' category, and 'cell part' (2409 unigenes, 19.88%) and 'cell' (2409 unigenes, 19.88%) were the most abundant terms. A further 20,072 unigenes were assigned to GO terms in the 'biological process' category, and the main terms were 'cellular process' (4329 unigenes, 21.56%) and 'single-organism process' (3326 unigenes, 16.57%). In addition, all unigenes were searched against the COG database for functional prediction and classification, and the results showed that 3865 unigenes (12.75%) could be assigned to 25 specific categories (Fig 3); 'signal transduction mechanisms' (567 unigenes, 14.67%) was the largest group, and 'cell motility' (5 unigenes, 0.13%) was the smallest group. Furthermore, KEGG annotation was used to divide unigenes into five KEGG pathways (cellular processes, environmental information processing, genetic information processing, metabolism, and organismal systems; Fig 4). Most unigenes were assigned to the 'processes' branch, and 'global and overview maps' (1251 unigenes, 28.07%) was the most highly represented term.

### Pheromone biosynthesis-activating neuropeptide receptor (PBANR)

The biosynthesis of Type-I sex pheromones in female moths has been shown to be regulated by a C-terminally amidated 33 amino acid neuropeptide termed PBAN that is released from the subesophageal ganglion in the brain and transported through the hemolymph to the PG [47–48]. The binding of PBAN to its receptor in the PG cell membrane will induce the opening of $Ca^{2+}$ channels causing the influx of extracellular $Ca^{2+}$, which then initiates sex pheromone production [49–50]. PBANR, a G protein-coupled receptor (GPCR), was first cloned from the PG of *Helicoverpa zea* [51]. PBANR has since been identified in *Bombyx mori* [52] and other Lepidoptera species [49, 53]. PBANRs exist as PBANR multiple isoforms (PBANR-As, -A, -B, and -C) based on alternative splicing of the C-terminus [54]. The various isoforms play different functional roles in the ligand-induced internalization [55], a phase of GPCR feedback regulation and desensitization in diverse moth species [56–57]. Herein, we identified a single

**Table 1. Summary of sequencing results.**

| | Raw data | | | Clean data | | |
|---|---|---|---|---|---|---|
| | Repeat 1 | Repeat 2 | Repeat 3 | Repeat 1 | Repeat 2 | Repeat 3 |
| **Read number** | 63,881,910 | 54,395,274 | 58,219,720 | 60,708,992 | 51,561,536 | 55,208,486 |
| **Base number** | 9,646,168,410 | 8,213,686,374 | 8,791,177,720 | 9,000,405,945 | 7,640,975,358 | 8,189,668,630 |
| **Q20 (%)** | 97.11 | 96.94 | 97.03 | 98.27 | 98.18 | 98.24 |
| **Q30 (%)** | 93.08 | 92.73 | 92.98 | 94.92 | 94.71 | 94.92 |
| **GC (%)** | 46.69 | 47.02 | 44.4 | 46.57 | 46.87 | 44.26 |

https://doi.org/10.1371/journal.pone.0227666.t001

PBANR in the *S. insularis* PG transcriptome that is 84% identical to *Mamestra brassicae* PBANR isoform B (ARO85772.1) and is very low in abundance (0.56 FPKM; Table 2 and S1 Text). The number of PBANR-encoding genes in the *S. insularis* PG was in accordance with *Plutella xylostella* [25], *Agrotis segetum* [58], and *Agrotis ipsilon* [59]. In addition, previous studies identified three isoforms of PBANR in *Ostrinia nubilalis* [60] and *Mamestra brassicae* [61]. However, we did not discover other isoforms of PBANR in our transcriptomic data, which may be explained by lower expression levels in *S. insularis*.

## Acetyl-CoA carboxylase (ACC)

The first step of saturated long-chain fatty acid biosynthesis is the ATP-dependent carboxylation of acetyl-CoA to malonyl-CoA catalyzed by ACC, a rate-limiting enzyme [13–14]. In the *S. insularis* PG transcriptome, we identified two ACCs with lengths of 723 and 7616 bp (Table 2 and S1 Text), similar to the numbers reported previously for other moth species (two in *A. ipsilon* [59], one in *P. xylostella* [25], and one in *A. segetum* [58]). *SinsACC1* with an ORF of 399 bp encodes for an ACC with 63% amino acid identity with the ACC of *Amyelois transitella* (XP_013185423.1), and *SinsACC2* has an intact ORF of 7101 bp that shares high amino

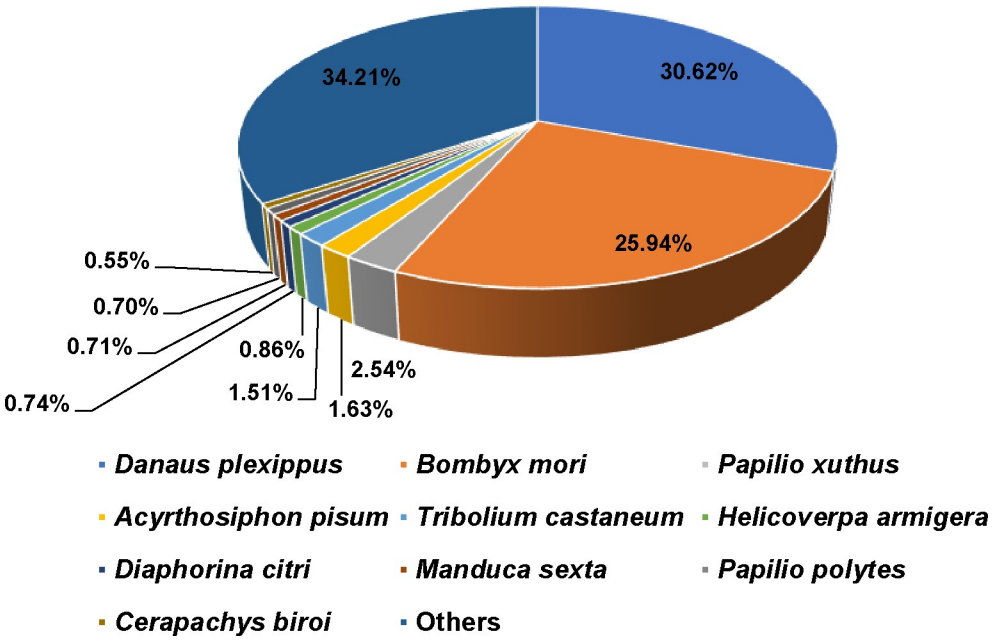


**Fig 1. Species distribution based on homology searches of *S. insularis* unigenes against the NCBI Nr protein database.**

https://doi.org/10.1371/journal.pone.0227666.g001

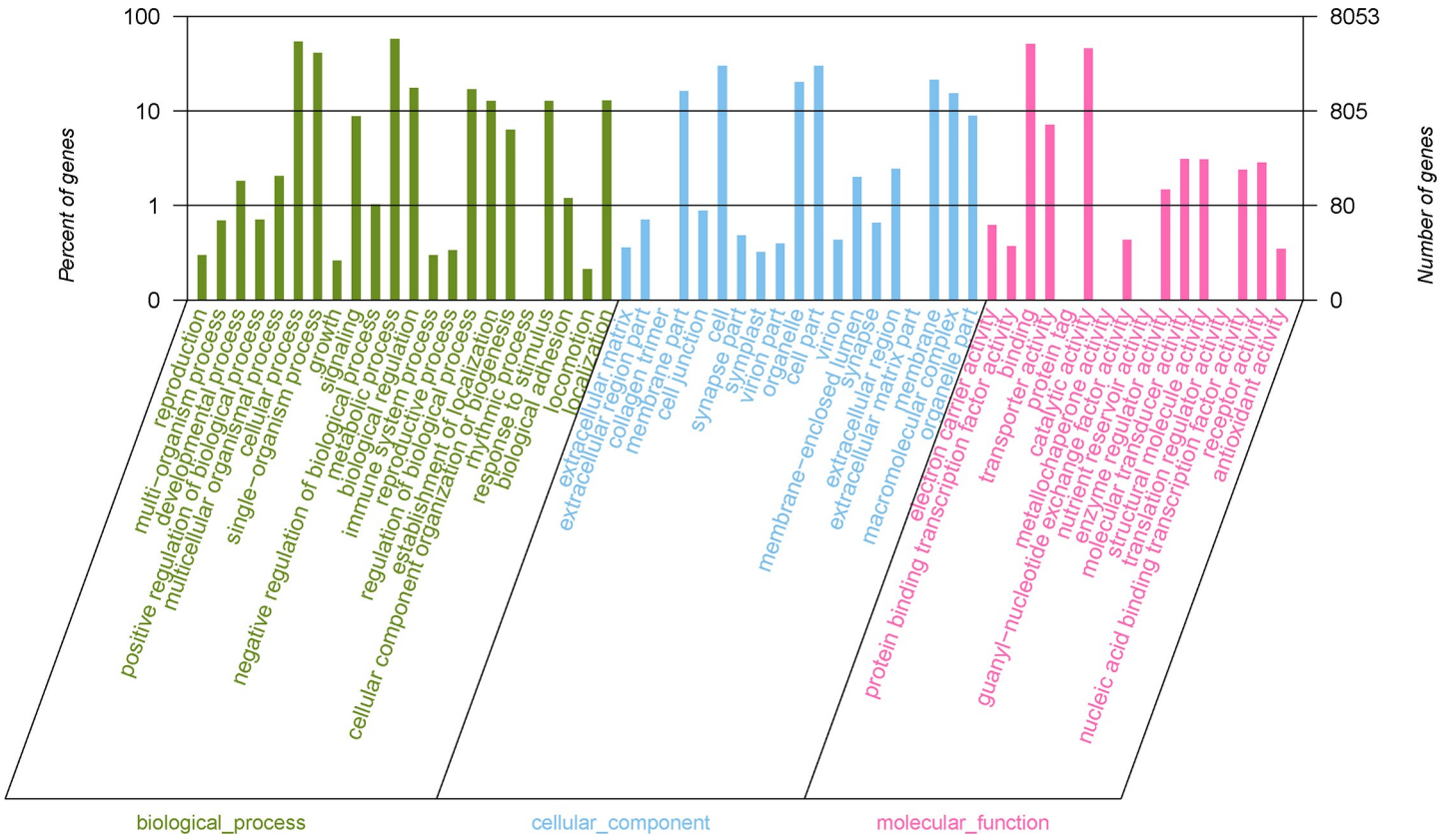


**Fig 2. GO classification of *S. insularis* unigenes.**

https://doi.org/10.1371/journal.pone.0227666.g002

acid identity (90%) with the ACC of *Papilio polytes* (XP_013146614.1). The RT-qPCR results (Fig 5) showed that *SinsACC1* was more strongly expressed in the antennae than in the other tissues, whereas *SinsACC2* was mainly expressed in the PG. However, both were present in low abundance (3.6 and 28.33 FPKM) in the *S. insularis* PG transcriptome. It was reported that the plastid-specific ACC is inhibited by herbicides that target the eukaryotic form of the enzyme in monocotyledonous plants [62–64]. Eliyahu et al. (2003) subsequently demonstrated that the herbicide diclofop inhibits PBAN-activated sex pheromone production in *Helicoverpa zea*, thereby implicating ACC plays a key regulatory role in fatty acid biosynthesis [65], which provides a basis for the development of a new pest control method based on disruption of sex pheromone production in females.

## Fatty acid synthase (FAS)

FAS is the multifunctional protein that catalyzes acetyl-CoA, malonyl-CoA, and NADPH through-multienzyme complex that catalyzes the synthesis of long-chain fatty acids. Labeling studies demonstrated that palmitic acid (C16) and stearic acid (C18) are the FAS products in most moth PGs [15, 66–67]. Herein, we identified five FASs with lengths ranging from 301 bp to 8170 bp in the *S. insularis* PG transcriptome (Table 2 and S1 Text), These results are similar to those reported for other insects, with six and three FASs in *A. segetum* [58] and *Sesamia inferens* [68], respectively. Among the five FASs, only *SinsFAS2* has an intact ORF. BLASTX results showed that FASs share high sequence similarity with Lepidoptera FASs in the NCBI

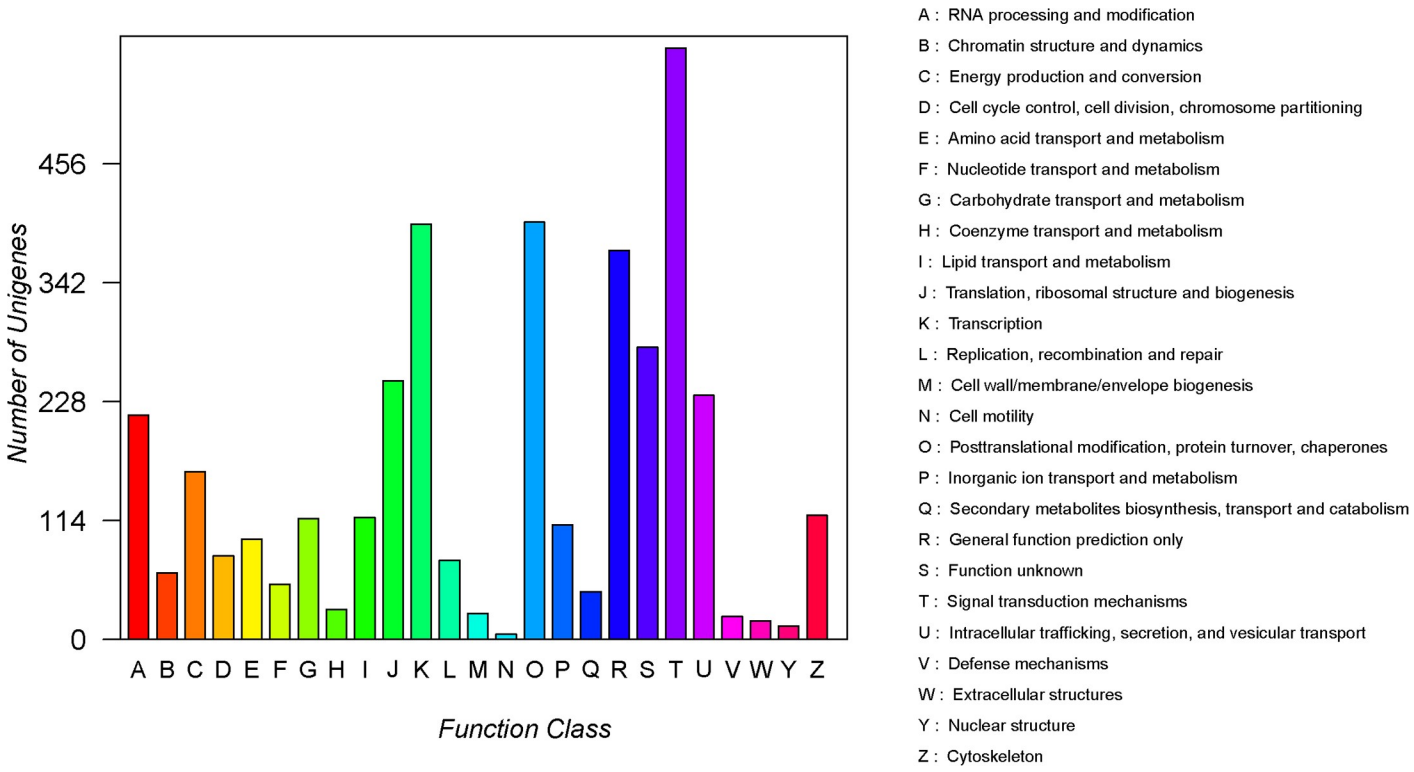


**Fig 3. COG classification of *S. insularis* unigenes.**

https://doi.org/10.1371/journal.pone.0227666.g003

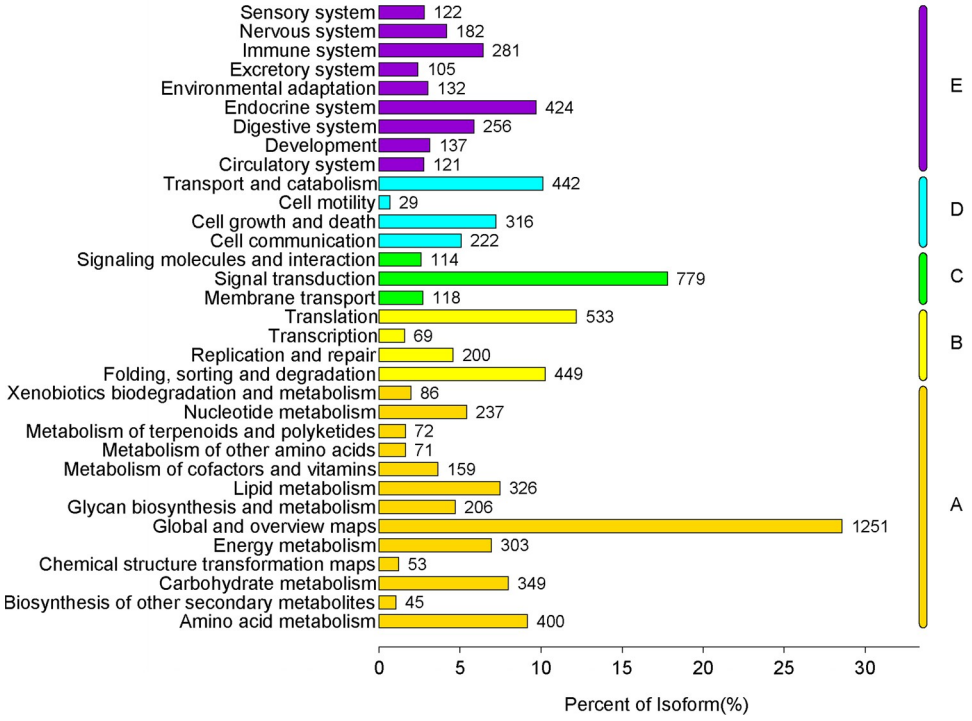


**Fig 4. KEGG classification of *S. insularis* unigenes.**

https://doi.org/10.1371/journal.pone.0227666.g004

**Table 2. Putative sex pheromone biosynthesis-related genes identified in the *S. insularis* pheromone gland transcriptome.**

| Name | Gene length (bp) | ORF length (bp) | Intact ORF | FPKM value | Best BLASTX match | | | | | |
|---|---|---|---|---|---|---|---|---|---|---|
| | | | | | Function | ACC number | Species | Score | E-value | Identity |
| **PBANR** | | | | | | | | | | |
| SinsPBANR | 1538 | 1224 | Yes | 0.56 | pheromone biosynthesis activating neuropeptide receptor isoform B | ARO85772.1 | *Mamestra brassicae* | 726 | 0 | 84% |
| **ACC** | | | | | | | | | | |
| SinsACC1 | 723 | 399 | No | 3.60 | PREDICTED: acetyl-CoA carboxylase | XP_013185423.1 | *Amyelois transitella* | 164 | 2E-42 | 63% |
| SinsACC2 | 7616 | 7101 | Yes | 28.33 | PREDICTED: acetyl-CoA carboxylase isoform X3 | XP_013146614.1 | *Papilio polytes* | 8781 | 0 | 90% |
| **FAS** | | | | | | | | | | |
| SinsFAS1 | 312 | 273 | No | 0.28 | fatty acid synthase | BAM19658.1 | *Papilio xuthus* | 153 | 3E-42 | 88% |
| SinsFAS2 | 8170 | 7173 | Yes | 90.41 | fatty acid synthase | AGR49310.1 | *Agrotis ipsilon* | 3623 | 0 | 81% |
| SinsFAS3 | 301 | 87 | No | 1.00 | PREDICTED: fatty acid synthase | XP_013141731.1 | *Papilio polytes* | 177 | 2E-49 | 85% |
| SinsFAS4 | 459 | 441 | No | 0.42 | fatty acid synthase 1 | AKD01760.1 | *Helicoverpa assulta* | 209 | 5E-65 | 62% |
| SinsFAS5 | 310 | 135 | No | 0.59 | fatty acid synthase-like | XP_021208123.1 | *Bombyx mori* | 164 | 4E-47 | 69% |
| **DES** | | | | | | | | | | |
| SinsDES1 | 244 | 225 | Yes | 1.81 | PREDICTED: acyl-CoA Delta(11) desaturase-like | XP_011561954.1 | *Plutella xylostella* | 134 | 2E-36 | 77% |
| SinsDES2 | 449 | 267 | Yes | 1.15 | acyl-CoA Delta(11) desaturase-like | XP_026752209.1 | *Galleria mellonella* | 168 | 4E-48 | 80% |
| SinsDES3 | 864 | 825 | No | 0.71 | acyl-CoA delta-11 desaturase | AAL16642.1 | *Argyrotaenia velutinana* | 394 | 5E-135 | 63% |
| SinsDES4 | 350 | 228 | No | 1.20 | stearoyl-CoA desaturase 5-like | XP_026757907.1 | *Galleria mellonella* | 171 | 2E-49 | 75% |
| SinsDES5 | 305 | 192 | No | 0.86 | stearoyl-CoA desaturase 5-like | XP_021195328.1 | *Helicoverpa armigera* | 186 | 5E-56 | 80% |
| SinsDES6 | 1278 | 1002 | Yes | 65.89 | desaturase | ARD71185.1 | *Spodoptera exigua* | 496 | 1E-172 | 70% |
| SinsDES7 | 1200 | 996 | Yes | 4.82 | acyl-CoA Delta(11) desaturase-like | XP_028166624.1 | *Ostrinia furnacalis* | 531 | 0 | 78% |
| SinsDES8 | 2500 | 1032 | Yes | 361.30 | acyl-CoA Delta(11) desaturase | XP_028982113.1 | *Diachasma alloeum* | 345 | 6E-108 | 52% |
| SinsDES9 | 2947 | 1143 | Yes | 5.42 | desaturase | AAQ74260.1 | *Spodoptera littoralis* | 590 | 0 | 74% |
| SinsDES10 | 7148 | 1962 | Yes | 3.36 | acyl-CoA-delta9-3a-desaturase | ABX71810.1 | *Dendrolimus punctatus* | 628 | 0 | 87% |
| SinsDES11 | 911 | 393 | Yes | 1.15 | putative C-5 sterol desaturase | KPJ05936.1 | *Papilio machaon* | 395 | 4E-134 | 81% |
| SinsDES12 | 483 | 111 | Yes | 1.47 | fatty acyl desaturase | AHW98356.1 | *Cydia pomonella* | 98.6 | 2E-21 | 77% |
| SinsDES13 | 1476 | 984 | Yes | 22.89 | desaturase | AIM40219.1 | *Cydia pomonella* | 581 | 0 | 85% |
| SinsDES14 | 1435 | 1128 | Yes | 0.41 | desaturase | AIM40222.1 | *Cydia pomonella* | 638 | 0 | 80% |
| SinsDES15 | 1563 | 966 | Yes | 86.74 | sphingolipid delta(4)-desaturase DES1 | XP_004930794.1 | *Bombyx mori* | 612 | 0 | 89% |
| SinsDES16 | 1484 | 1017 | Yes | 1.66 | desaturase | ARD71181.1 | *Spodoptera exigua* | 515 | 2E-179 | 72% |
| SinsDES17 | 2225 | 1062 | Yes | 426.07 | acyl-CoA Delta(11) desaturase-like isoform X1 | XP_021183600.1 | *Helicoverpa armigera* | 624 | 0 | 82% |
| **ACO** | | | | | | | | | | |
| SinsACO1 | 405 | 363 | No | 1.10 | probable peroxisomal acyl-coenzyme A oxidase 1 | XP_026758799.1 | *Galleria mellonella* | 215 | 1E-63 | 73% |
| SinsACO2 | 2480 | 2013 | Yes | 42.90 | PREDICTED: probable peroxisomal acyl-coenzyme A oxidase 1 | XP_013188704.1 | *Amyelois transitella* | 1166 | 0 | 85% |
| SinsACO3 | 2792 | 2070 | Yes | 1.92 | peroxisomal acyl-coenzyme A oxidase 3 | XP_022819471.1 | *Spodoptera litura* | 1181 | 0 | 80% |
| SinsACO4 | 3173 | 2097 | Yes | 11.84 | peroxisomal acyl-CoA oxidase 3 | AID66678.1 | *Agrotis segetum* | 1165 | 0 | 77% |
| SinsACO5 | 375 | 189 | No | 0.57 | PREDICTED: probable peroxisomal acyl-coenzyme A oxidase 1 | XP_014367103.1 | *Papilio machaon* | 236 | 5E-77 | 89% |
| SinsACO6 | 2104 | 1899 | No | 26.85 | probable peroxisomal acyl-coenzyme A oxidase 1 isoform X1 | XP_022821900.1 | *Spodoptera litura* | 964 | 0 | 73% |
| SinsACO7 | 1919 | 1893 | No | 9.16 | PREDICTED: probable peroxisomal acyl-coenzyme A oxidase 1 | XP_013149571.1 | *Papilio polytes* | 992 | 0 | 75% |
| SinsACO8 | 279 | 243 | No | 0.00 | probable peroxisomal acyl-coenzyme A oxidase 1 | XP_021195539.1 | *Helicoverpa armigera* | 181 | 5E-52 | 90% |
| **ACD** | | | | | | | | | | |

(*Continued*)

**Table 2.** (Continued)

| Name | Gene length (bp) | ORF length (bp) | Intact ORF | FPKM value | Best BLASTX match | | | | | |
|---|---|---|---|---|---|---|---|---|---|---|
| | | | | | Function | ACC number | Species | Score | E-value | Identity |
| SinsACD1 | 1214 | 768 | Yes | 19.22 | 3-hydroxyacyl-CoA dehydrogenase type-2 | XP_026727946.1 | *Trichoplusia ni* | 464 | 1E-161 | 89% |
| SinsACD2 | 3886 | 1902 | Yes | 214.36 | very long-chain-specific acyl-CoA dehydrogenase, mitochondrial isoform X1 | XP_026737732.1 | *Trichoplusia ni* | 944 | 0 | 80% |
| SinsACD3 | 1056 | 774 | Yes | 3.34 | 3-hydroxyacyl-CoA dehydrogenase type-2-like isoform X1 | XP_026761478.1 | *Galleria mellonella* | 429 | 7E-149 | 79% |
| SinsACD4 | 1252 | 933 | Yes | 105.77 | hydroxyacyl-coenzyme A dehydrogenase, mitochondrial-like | XP_022822785.1 | *Spodoptera litura* | 581 | 0 | 89% |
| SinsACD5 | 1547 | 1266 | Yes | 145.78 | short/branched-chain-specific acyl-CoA dehydrogenase, mitochondrial | XP_023946257.1 | *Bicyclus anynana* | 808 | 0 | 92% |
| SinsACD6 | 2320 | 1830 | Yes | 11.66 | PREDICTED: acyl-CoA dehydrogenase family member 9, mitochondrial | XP_013192619.1 | *Amyelois transitella* | 902 | 0 | 69% |
| SinsACD7 | 3306 | 1236 | Yes | 12.58 | short-chain-specific acyl-CoA dehydrogenase, mitochondrial-like isoform X1 | XP_028162581.1 | *Ostrinia furnacalis* | 697 | 0 | 81% |
| SinsACD8 | 2324 | 1275 | Yes | 210.50 | probable medium-chain-specific acyl-CoA dehydrogenase, mitochondrial | NP_001298861.1 | *Papilio xuthus* | 712 | 0 | 84% |
| SinsACD9 | 4692 | 1224 | Yes | 17.89 | short-chain-specific acyl-CoA dehydrogenase, mitochondrial | XP_026489065.1 | *Vanessa tameamea* | 709 | 0 | 89% |
| **ECH** | | | | | | | | | | |
| SinsECH1 | 1207 | 990 | Yes | 10.81 | PREDICTED: probable enoyl-CoA hydratase | XP_013137975.1 | *Papilio polytes* | 484 | 2E-168 | 82% |
| SinsECH2 | 1321 | 303 | Yes | 2.54 | enoyl-CoA hydratase domain-containing protein 3, mitochondrial isoform X2 | XP_022822616.1 | *Spodoptera litura* | 393 | 3E-85 | 82% |
| SinsECH3 | 1439 | 894 | Yes | 13.68 | enoyl-CoA hydratase domain-containing protein 2, mitochondrial | XP_028167557.1 | *Ostrinia furnacalis* | 445 | 1E-152 | 79% |
| **HAD** | | | | | | | | | | |
| SinsHAD1 | 1214 | 768 | Yes | 19.22 | 3-hydroxyacyl-CoA dehydrogenase type-2 | XP_026727946.1 | *Trichoplusia ni* | 464 | 1E-161 | 89% |
| SinsHAD2 | 1056 | 774 | Yes | 3.34 | 3-hydroxyacyl-CoA dehydrogenase type-2-like isoform X1 | XP_026761478.1 | *Galleria mellonella* | 429 | 7E-149 | 79% |
| SinsHAD3 | 1252 | 933 | Yes | 105.77 | hydroxyacyl-CoA dehydrogenase | AID66694.1 | *Agrotis segetum* | 575 | 0 | 87% |
| **KAT** | | | | | | | | | | |
| SinsKAT1 | 1395 | 1194 | Yes | 10.21 | 3-ketoacyl-CoA thiolase, mitochondrial-like | XP_028176321.1 | *Ostrinia furnacalis* | 491 | 5E-169 | 63% |
| **FAR** | | | | | | | | | | |
| SinsFAR1 | 1805 | 1545 | No | 5.57 | PREDICTED: fatty acyl-CoA reductase 1-like | XP_013185409.1 | *Amyelois transitella* | 761 | 0 | 71% |
| SinsFAR2 | 1867 | 1692 | No | 1.62 | fatty acyl reductase 5 | ATJ44463.1 | *Helicoverpa armigera* | 816 | 0 | 73% |
| SinsFAR3 | 2335 | 1875 | Yes | 33.44 | fatty acyl-CoA reductase 2 | ADI82775.1 | *Ostrinia nubilalis* | 992 | 0 | 80% |
| SinsFAR4 | 457 | 354 | No | 0.85 | fatty acyl reductase | ARD71192.1 | *Spodoptera exigua* | 193 | 3E-56 | 77% |
| SinsFAR5 | 967 | 723 | No | 0.56 | fatty acyl-CoA reductase 1 | XP_021197389.1 | *Helicoverpa armigera* | 360 | 4E-118 | 57% |
| SinsFAR6 | 2395 | 1494 | Yes | 476.06 | fatty acyl reductase | AID66655.1 | *Agrotis segetum* | 441 | 1E-143 | 46% |
| SinsFAR7 | 2040 | 1575 | Yes | 15.48 | putative fatty acyl-CoA reductase CG5065 | XP_004925992.1 | *Bombyx mori* | 900 | 0 | 84% |
| SinsFAR8 | 2910 | 1578 | Yes | 0.60 | putative fatty acyl-CoA reductase CG5065 | XP_026483533.1 | *Vanessa tameamea* | 1019 | 0 | 92% |
| SinsFAR9 | 1820 | 1605 | No | 9.83 | fatty acyl reductase | ARD71186.1 | *Spodoptera exigua* | 726 | 0 | 73% |
| SinsFAR10 | 1807 | 1560 | Yes | 2.70 | fatty acyl-CoA reductase 1 | XP_021197389.1 | *Helicoverpa armigera* | 783 | 0 | 73% |
| SinsFAR11 | 1875 | 1500 | Yes | 65.72 | putative fatty acyl-CoA reductase CG5065 | XP_028038252.1 | *Bombyx mandarina* | 792 | 0 | 73% |
| SinsFAR12 | 2448 | 1590 | Yes | 35.68 | putative fatty acyl-CoA reductase CG5065 | XP_022835056.1 | *Spodoptera litura* | 635 | 0 | 64% |
| SinsFAR13 | 4732 | 1533 | Yes | 24.19 | putative fatty acyl-CoA reductase CG8306 | XP_004930778.1 | *Bombyx mori* | 855 | 0 | 79% |
| **AD** | | | | | | | | | | |
| SinsAD1 | 1221 | 975 | Yes | 28.73 | alcohol dehydrogenase | BAR64763.1 | *Ostrinia furnacalis* | 529 | 0 | 80% |

(*Continued*)

**Table 2.** (Continued)

| Name | Gene length (bp) | ORF length (bp) | Intact ORF | FPKM value | Best BLASTX match | | | | | |
|---|---|---|---|---|---|---|---|---|---|---|
| | | | | | Function | ACC number | Species | Score | E-value | Identity |
| SinsAD2 | 1746 | 813 | Yes | 13.93 | alcohol dehydrogenase AD1 | AII21999.1 | *Sesamia inferens* | 360 | 4E-118 | 66% |
| SinsAD3 | 2923 | 1131 | Yes | 35.49 | alcohol dehydrogenase class-3 | XP_021189392.1 | *Helicoverpa armigera* | 658 | 0 | 94% |
| SinsAD4 | 1395 | 1059 | Yes | 7.76 | alcohol dehydrogenase | BAR64764.1 | *Ostrinia furnacalis* | 579 | 0 | 80% |
| SinsAD5 | 1209 | 750 | Yes | 37.20 | alcohol dehydrogenase AD2 | AKQ06148.1 | *Cydia pomonella* | 327 | 7E-108 | 71% |
| **AR** | | | | | | | | | | |
| SinsAR1 | 853 | 807 | No | 6.56 | aldo-keto reductase AKR2E4-like | XP_028160456.1 | *Ostrinia furnacalis* | 377 | 2E-128 | 69% |
| SinsAR2 | 1125 | 1011 | Yes | 27.65 | aldo-keto reductase AKR2E4-like | XP_028177948.1 | *Ostrinia furnacalis* | 506 | 5E-177 | 71% |
| SinsAR3 | 1738 | 1092 | Yes | 25.10 | aldo-keto reductase AKR2E4-like | XP_022830935.1 | *Spodoptera litura* | 553 | 0 | 75% |
| SinsAR4 | 1252 | 1032 | Yes | 26.15 | PREDICTED: aldo-keto reductase AKR2E4-like | XP_013136681.1 | *Papilio polytes* | 498 | 8E-174 | 70% |
| SinsAR5 | 1242 | 987 | Yes | 125.24 | aldehyde reductase 7 | ATJ44502.1 | *Helicoverpa armigera* | 507 | 1E-177 | 71% |
| **ATF** | | | | | | | | | | |
| SinsATF1 | 1775 | 1269 | Yes | 23.49 | acetyl-CoA acetyltransferase, mitochondrial | XP_028157143.1 | *Ostrinia furnacalis* | 777 | 0 | 89% |
| SinsATF2 | 379 | 285 | Yes | 0.47 | PREDICTED: acetyl-CoA acetyltransferase, mitochondrial isoform X2 | XP_013192024.1 | *Amyelois transitella* | 177 | 7E-51 | 79% |

https://doi.org/10.1371/journal.pone.0227666.t002

Nr protein database (>60%). The FPKM analysis showed that *SinsFAS2* displayed the highest expression level (90.41 FPKM) in the *S. insularis* PG.

## Desaturase (DES)

Double bonds are introduced into the fatty acid chain at specific positions by a variety of desaturases [69]. Three putative sex pheromone compounds of *S. insularis* were identified as Z3-14:OAc, E3-14:OAc, and Z5-12:OAc, which are unsaturated fatty acids with acetate esters as the functional group. It is therefore reasonable to assume that the saturated fatty acid precursor of *S. insularis* sex pheromones is palmitic acid (C16), which is desaturated by Δ5-desaturase and Δ9-desaturase to form the precursors Z/E5-16:acyl-CoA and Z9-16:acyl-CoA in the production of two major (Z3-14:OAc and E3-14:OAc) and one minor (Z5-12:OAc) sex pheromone component, respectively (Figs 6 and 7). From the *S. insularis* PG transcriptome, we identified 17 putative DESs with lengths ranging from 244 to 7148 bp (Table 2 and S1 Text). The number of DESs identified in *S. insularis* was more than that in *A. ipsilon* [59], *P. xylostella* [25], and *A. segetum* [58]. Of these DESs, the identity of the best BLASX match in the NCBI NR database ranged from 52% to 89%. Notably, *SinsDES15* identified in the *S. insularis* transcriptome shared the highest identity (89%), comparable with *DES1* in *Bombyx mori* (XP_004930794.1). Of the 17 DESs, nine DES sequences were either less than 1000 bp, or no common sites were found for computing distances; thus, we only used the remaining eight *S. insularis* DES sequences to construct our phylogenetic tree (Fig 8). In the tree, *SinsDES13* and *SinsDES16* are clustered in the 'Δ11-desaturases' clade. The *SinsDES17* sequence shares high sequence homology with 'Δ9-desaturases', and it clusters with other enzymes also possessing the NPVE motif. The remaining DESs clustered into the 'other desaturases' ortholog clade. The qRT-PCR results (Fig 5) revealed that *SinsDES6* and *SinsDES8* were highly expressed in *S. insularis* PG compared with the other tissues, suggesting that they may play roles in *S. insularis* sex pheromone production. The other five DESs (*SinsDES1*, *SinsDES3*, *SinsDES4*, *SinsDES6*, and *SinsDES7*) were expressed at significantly higher levels in antennae than in other tissues.

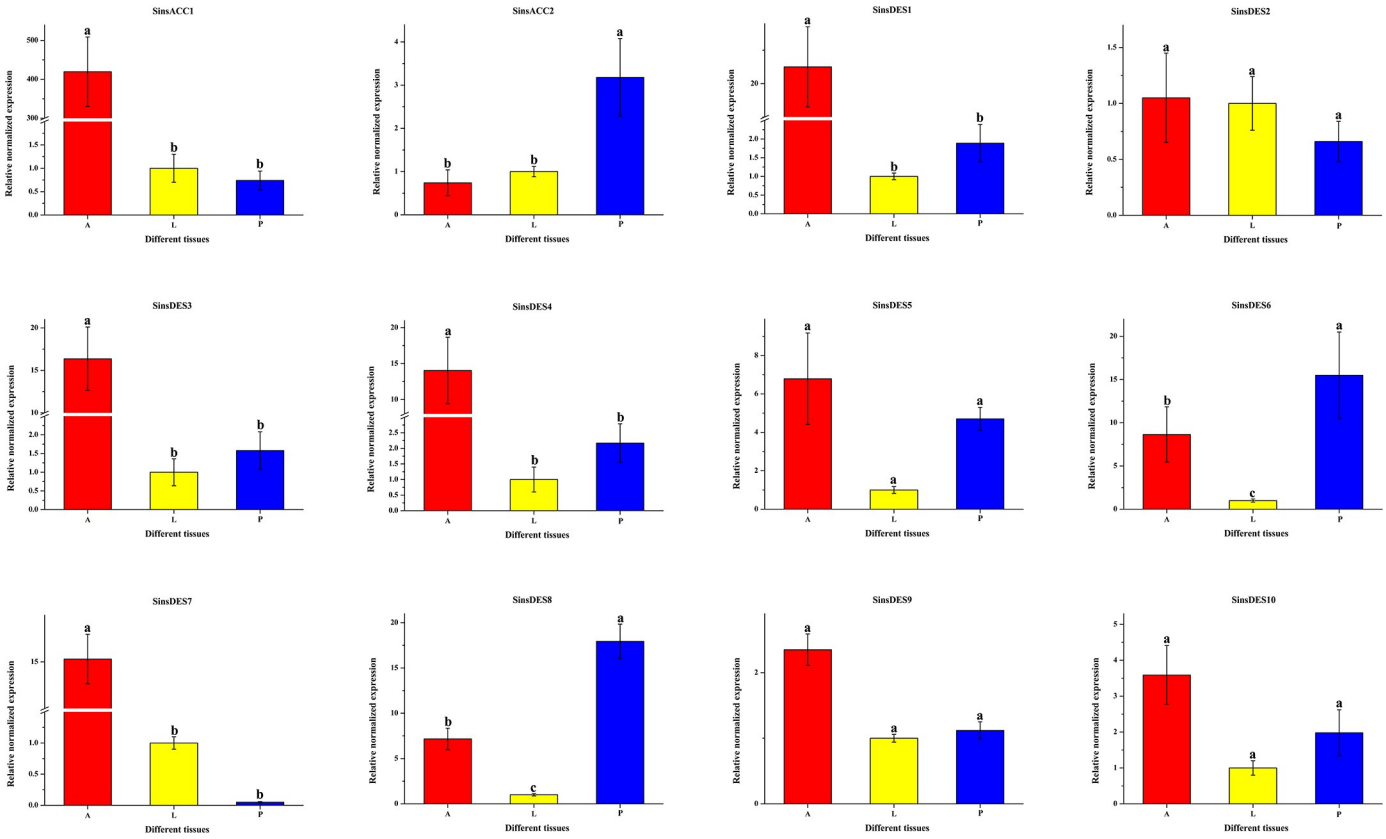


**Fig 5. Expression profiles of putative ACCs and DESs in different *S. insularis* tissues.** A, antennae; L, legs; P, pheromone glands. Actin was used as an internal reference gene for normalizing target gene expression. Standard errors are represented by error bars, and different lowercase letters (a–c) above bars denote significant differences ($p < 0.05$).

https://doi.org/10.1371/journal.pone.0227666.g005

All DESs except *SinsDES8* and *SinsDES17* were present at low abundance (from 0.41 to 86.74 FPKM) in the *S. insularis* PG transcriptome. DESs play important roles in the generation of structural diversity in Lepidopteran sex pheromone biosynthesis, owing to the evolution of diverse enzymatic properties [22]. Based on the most likely sex pheromone biosynthetic pathways in *S. insularis*, both the Δ5- and Δ9-desaturase are likely involved, but it is not clear which of the 17 desaturase genes identified in our study encode these enzymes. Further biochemical analyses of these desaturases are required to determine which ones are involved in pheromone biosynthesis.

## β-oxidation enzymes

After a specific Δ5 or Δ9 double bond is introduced into palmitic acid to form a fatty acyl CoA precursor, the chain of the precursors is then shortened sequentially via a β-oxidation catabolic process to generate different shorter chain pheromone precursors (14C and 12C). Each cycle of β-oxidation involves four reactions: (1) acyl-CoA oxidases (ACOs, in peroxisomes) and acyl-CoA dehydrogenases (ACDs, in mitochondria) act on acyl-CoA to form *E*2-enoyl-CoA; (2) *E*2-enoyl-CoA is reversibly hydrated by enoyl-CoA hydratase (ECH) to form L-3-hydroxyacyl-CoA; (3) L-3-hydroxyacyl-CoA dehydrogenase (HAD) catalyzes the reversible dehydrogenation of L-3-hydroxyacyl-CoA to 3-ketoacyl-CoA; and (4) 3-ketoacyl-CoA is cleaved by 3-ketoacyl-CoA thiolase (KAT) [37, 70–72]. In the *S. insularis* PG transcriptome, we identified

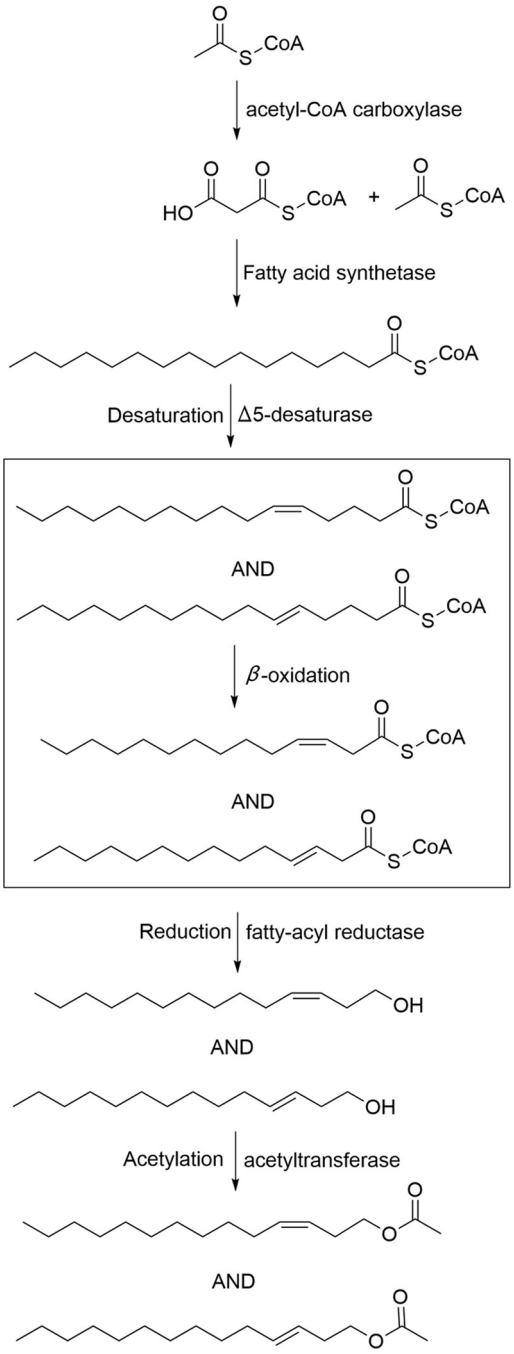


**Fig 6. Putative biosynthesis pathway of the sex pheromone components Z3-14:OAc and E3-14:OAc in *S. insularis*.** The saturated fatty acid precursor palmitic acid (16:0) is desaturated by Δ5-desaturase to form the precursor Z/E5-16: acyl-CoA in the production of two major pheromone components (Z3-14:OAc and E3-14:OAc).

https://doi.org/10.1371/journal.pone.0227666.g006

eight ACO genes, nine ACD genes, three ECH genes, three HAD genes, and one KAT gene (Table 2 and S1 Text). The derived protein sequences of these 24 transcripts share 63–92%

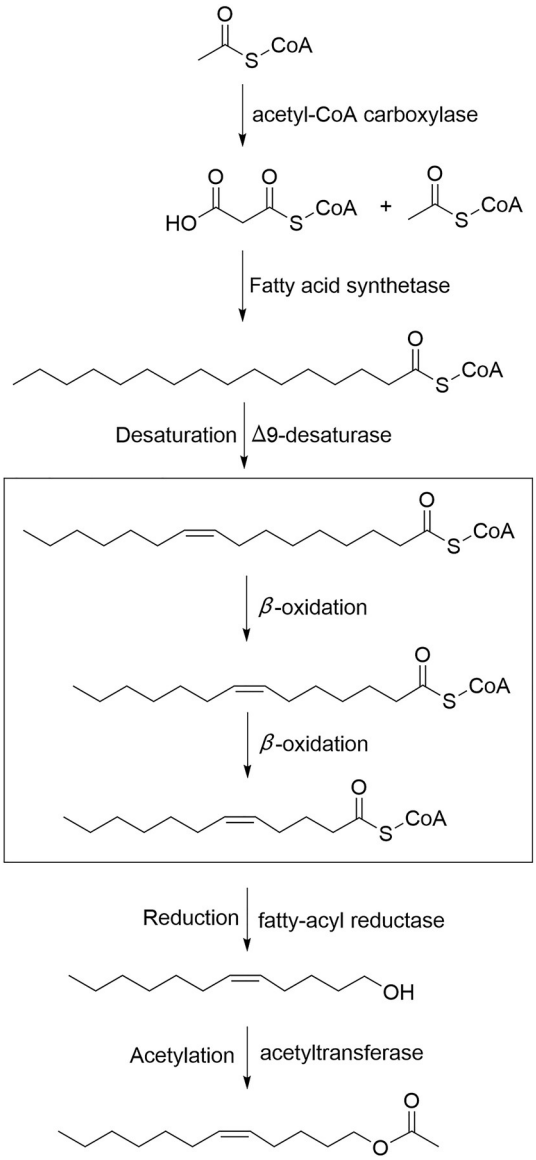


**Fig 7. Putative biosynthesis pathway of the sex pheromone component Z5-12:OAc in *S. insularis*.** The saturated fatty acid precursor palmitic acid (16:0) is desaturated by Δ9-desaturase to form the precursor Z9-16:acyl-CoA in the production of the minor pheromone component Z5-12:OAc.

https://doi.org/10.1371/journal.pone.0227666.g007

amino acid identity with their homologs in other insects. All transcripts were present in low abundance (from 0 to 214.36 FPKM) in the *S. insularis* PG.

## Fatty acyl-CoA reductase (FAR)

Chain-shortened fatty acyl CoA precursors are reduced to the corresponding alcohols by alcohol-generating FARs. Fatty alcohols can serve as sex pheromone components in many moths including *Plutella xylostella* [25]. Herein, we detected 13 transcripts homologous to putative FAR genes in the *S. insularis* PG transcriptome (Table 2 and S1 Text), similar to the number identified in other moth species (13 in *A. ipsilon* [59] and 10 in *A. segetum* [58]). Among them, *SinsFAR6* was expressed at the highest level (476.06 FPKM). The FARs in *S. insularis* encode

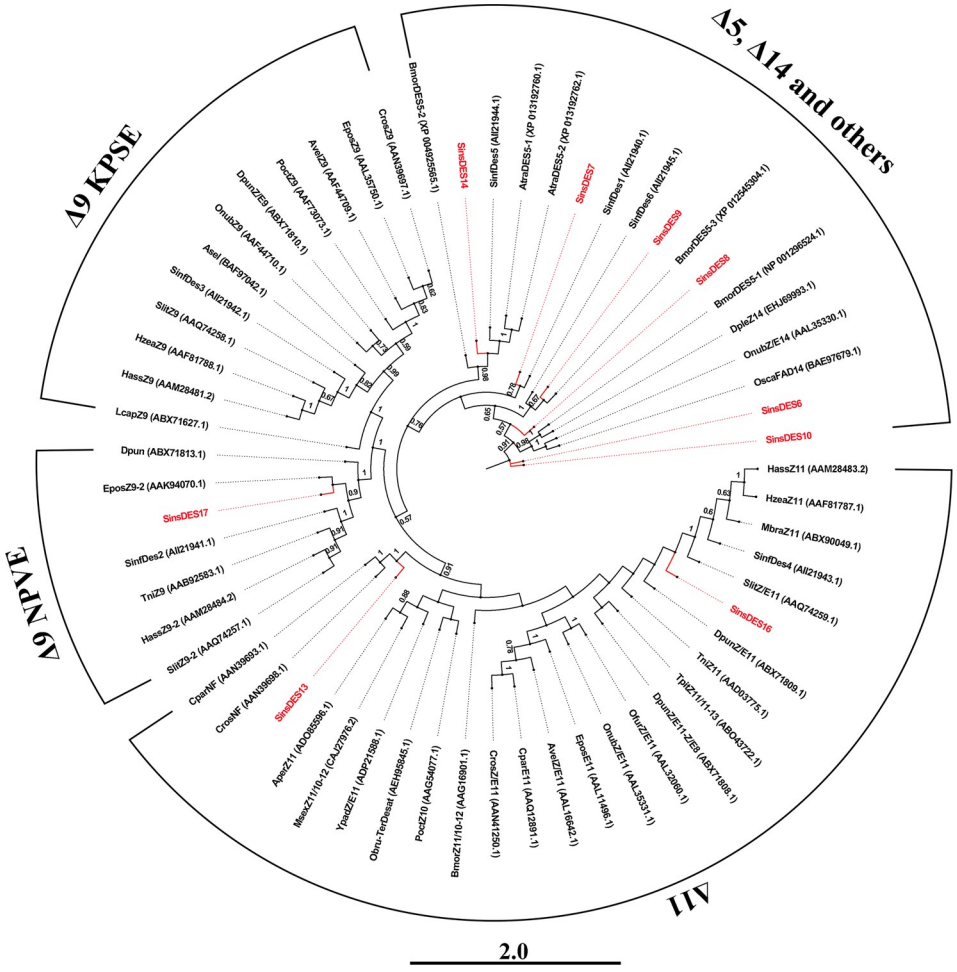


**Fig 8. Neighbor-joining phylogenetic tree of selected Lepidopteran DES enzymes.** The stability of nodes was assessed by bootstrap analysis with 1000 replicates, and only bootstrap values ≥0.5 are shown at the corresponding nodes. The scale bar represents 2.0 substitutions per site. *S. insularis* sequences are colored red.

https://doi.org/10.1371/journal.pone.0227666.g008

proteins shared 46–92% amino acid sequence identity with homologs in other Lepidoptera moths such as *B. mori*, *Helicoverpa armigera*, and *Spodoptera exigua*.

## Alcohol dehydrogenase (AD)

Fatty alcohols can also be used as pheromone intermediates to produce corresponding aldehydes by ADs [73]. In the *S. insularis* PG, five homologous full-length AD genes were identified (Table 2 and S1 Text). The number of AD-encoding genes in *S. insularis* was in accordance with *P. xylostella* [25] and *A. ipsilon* [59]. Two ADs (*SinsAD1* and *SinsAD4*) encode proteins that are homologous to ADs in *Ostrinia furnacalis* (BAR64763.1 and BAR64764.1) and share relatively high amino acid sequence identity (70%); *SinsAD2* encodes a protein sharing 66% identity with *Sesamia inferens* AD1 (AII21999.1), *SinsAD3* encodes a protein sharing 94% identity with the AD of *Helicoverpa armigera* (XP_021189392.1), and *SinsAD5* encodes a protein sharing 71% identity with the AD of *Cydia pomonella* (AKQ06148.1). FPKM value analysis revealed low expression levels in the *S. insularis* PG for all five ADs (FPKM <50).

### Aldehyde reductase (AR)

ARs are a group of the aldo-keto reductases that catalyze the reduction of fatty aldehydes to alcohols [74]. Whether ARs first produce aldehydes which are then converted to alcohols, or vice versa, is very difficult to distinguish in sex pheromone biosynthesis. Herein, we identified five AR genes in the *S. insularis* PG transcriptome, and four included intact ORFs (Table 2 and S1 Text). The number of ARs identified in *S. insularis* was less than that in *A. ipsilon* [59] and *P. xylostella* [25]. The deduced protein sequences of these five genes share high amino acid sequence identity (>60%) with their homologs in other Lepidoptera species, and all were expressed at low levels (from 6.56 to 125.24 FPKM) in the *S. insularis* PG.

### Acetyltransferase (ATF)

ATF catalyzes the conversion of fatty alcohols to acetate esters, and this is the final enzyme in the pheromone biosynthetic pathway of the *S. insularis*. Previous studies showed that ATF is found almost exclusively in the PG, and is active during the photophase and all adult stages [75–76]. ATF is microsomal and exhibits specificity for the Z isomer of 12-, 14-, and 16-carbon monounsaturated fatty alcohol substrates [29–30, 75–76]. However, the enzyme has not been identified at the gene level in any moth so far [58]. In the present study, we identified two transcripts predicted to encode ATFs in the *S. insularis* PG (Table 2 and S1 Text). The number of ATF-encoding genes in the *S. insularis* PG was in accordance with *P. xylostella* [25]. The BLASTX results revealed 89% and 79% amino acid sequence identity shared with putative ATFs of *Ostrinia furnacalis* and *Amyelois transitella* (XP_028157143.1 and XP_013192024.1), respectively. Both ATF transcripts were present at low abundance (23.49 and 0.47 FPKM) in the *S. insularis* PG.

## Supporting information

**S1 Table. Primers used for RT-qPCR analysis of ACCs and DESs in *S. insularis*.**
(DOCX)

**S1 Text. Nucleic acid sequences of all putative sex pheromone biosynthesis-related genes identified in the *S. insularis* pheromone gland transcriptome.**
(DOCX)

## Acknowledgments

The authors would like to thank Dr. Lili Ren and Dr. Yongliang Zhang for their suggestions and encouragement.

## Author Contributions

**Conceptualization:** Yuchao Yang, Jing Tao.

**Data curation:** Yuchao Yang, Jing Tao, Shixiang Zong.

**Formal analysis:** Yuchao Yang.

**Funding acquisition:** Shixiang Zong.

**Investigation:** Yuchao Yang.

**Methodology:** Yuchao Yang.

**Project administration:** Yuchao Yang, Jing Tao, Shixiang Zong.

**Resources:** Yuchao Yang, Shixiang Zong.

**Software:** Yuchao Yang.

**Supervision:** Jing Tao, Shixiang Zong.

**Validation:** Yuchao Yang, Jing Tao, Shixiang Zong.

**Visualization:** Yuchao Yang.

**Writing – original draft:** Yuchao Yang.

**Writing – review & editing:** Jing Tao, Shixiang Zong.

## References


1. Ando T, Inomata S, Yamamoto M. Lepidopteran sex pheromones. Top Curr Chem. 2004; 239: 51–96. https://doi.org/10.1007/b95449 PMID: 22160231
2. Witzgall P, Kirsch P, Cork A. Sex pheromones and their impact on pest management. J Chem Ecol. 2010; 36: 80–100. https://doi.org/10.1007/s10886-009-9737-y PMID: 20108027
3. McNeil JN. Behavioral ecology of pheromone-mediated communication in moths and its importance in the use of pheromone traps. Annu Rev Entomol. 1991; 36: 407–430.
4. Tillman JA, Seybold SJ, Jurenka RA, Blomquist GJ. Insect pheromones—an overview of biosynthesis and endocrine regulation. Insect Biochem Mol Biol. 1999; 29: 481–514. https://doi.org/10.1016/s0965-1748(99)00016-8 PMID: 10406089
5. Löfstedt C, Wahlberg N, Millar JG. Evolutionary patterns of pheromone diversity in lepidoptera. In: Allison JD, Cardé RT, editors. Pheromone communication in moths: evolution, behavior and application. Berkeley: University of California Press. 2016. pp. 43–78.
6. Löfstedt C, Hansson BS, Petersson E, Valeur P, Richards A. Pheromonal secretions from glands on the 5th abdominal sternite of hydropsychid and rhyacophilid caddisflies (Trichoptera). J Chem Ecol. 1994; 20:153–170. https://doi.org/10.1007/BF02065998 PMID: 24241706
7. Kozlov MV, Zhu JW, Philipp P, Francke W, Zvereva EL, Hansson BS, et al. Pheromone specificity in Eriocrania semipurpurella (Stephens) and E. sangii (Wood) (Lepidoptera: Eriocraniidae) based on chirality of semiochemicals. J Chem Ecol. 1996; 22: 431–454. https://doi.org/10.1007/BF02033647 PMID: 24227484
8. Raina AK, Wergin WP, Murphy CA, Erbe EF. Structural organization of the sex pheromone gland in Helicoverpa zea in relation to pheromone production and release. Arthropod Struct Dev. 2000; 29: 343–353. PMID: 18088939
9. Jurenka R. Insect pheromone biosynthesis. Top Curr Chem. 2004; 239: 97–132. https://doi.org/10.1007/b95450 PMID: 22160232
10. Matsumoto S. Molecular mechanisms underlying sex pheromone production in moths. Biosci Biotechnol Biochem. 2010; 74: 223–231. https://doi.org/10.1271/bbb.90756 PMID: 20139627
11. Moto K, Suzuki MG, Hull JJ, Kurata R, Takahashi S, Yamamoto M, et al. Involvement of a bifunctional fatty-acyl desaturase in the biosynthesis of the silkmoth, *Bombyx mori*, sex pheromone. Proc Natl Acad Sci USA. 2004; 101: 8631–8636. https://doi.org/10.1073/pnas.0402056101 PMID: 15173596
12. Park HY, Kim MS, Paek A, Jeong SE, Knipple DC. An abundant acyl-CoA (Δ9) desaturase transcript in pheromone glands of the cabbage moth, Mamestra brassicae, encodes a catalytically inactive protein. Insect Biochem Mol Biol. 2008; 38: 581–595. https://doi.org/10.1016/j.ibmb.2008.02.001 PMID: 18405835
13. Volpe JJ, Vagelos PR. Saturated fatty acid biosynthesis and its regulation. Annu Rev Biochem. 1973; 42: 21–60. https://doi.org/10.1146/annurev.bi.42.070173.000321 PMID: 4147183
14. Pape ME, Lopez-Casillas F, Kim KH. Physiological regulation of acetyl-CoA carboxylase gene expression: effects of diet, diabetes, and lactation on acetyl-CoA carboxylase mRNA. Arch Biochem Biophys. 1988; 267: 104–109. https://doi.org/10.1016/0003-9861(88)90013-6 PMID: 2904242
15. Bjostad LB, Roelofs WL. Biosynthesis of sex pheromone components and glycerolipid precursors from sodium [1–$^{14}$C] acetate in redbanded leafroller moth. J Chem Ecol. 1984; 10: 681–691. https://doi.org/10.1007/BF00994228 PMID: 24318604
16. Foster SP, Roelofs WL. Sex pheromone biosynthesis in the tortricid moth, Ctenopseustis herana (Felder & Rogenhofer). Arch Insect Biochem Physiol. 1996; 32: 135–147.

17. Wang HL, Liénard MA, Zhao CH, Wang CZ, Löfstedt C. Neofunctionalization in an ancestral insect desaturase lineage led to rare $\Delta^6$ pheromone signals in the Chinese tussah silkworm. Insect Biochem Mol Biol. 2010; 40: 742–751. https://doi.org/10.1016/j.ibmb.2010.07.009 PMID: 20691782

18. Löfstedt C, Bengtsson M. Sex pheromone biosynthesis of (E,E)-8,10-dodecadienol in codling moth Cydia pomonella involves E9 desaturation. J Chem Ecol. 1988; 14: 903–915. https://doi.org/10.1007/BF01018782 PMID: 24276140

19. Foster SP, Roelofs WL. Sex pheromone biosynthesis in the leafroller moth *Planotortix excessana* by Δ10 desaturation. Arch Insect Biochem Physiol. 1988; 8: 1–9.

20. Bjostad LB, Roelofs WL. Sex pheromone biosynthesis from radiolabeled fatty acids in the redbanded leafroller moth. J Biol Chem. 1981; 256: 7936–7940. PMID: 7021542

21. Zhao CH, Löfstedt C, Wang XY. Sex pheromone biosynthesis in the Asian corn borer Ostrinia furnacalis (II): Biosynthesis of (E)-and (Z)-12-tetradecenyl acetate involves Δ14 desaturation. Arch Insect Biochem Physiol. 1990; 15: 57–65.

22. Knipple DC, Rosenfield CL, Nielsen R, You KM, Jeong SE. Evolution of the integral membrane desaturase gene family in moths and flies. Genetics. 2002; 162: 1737–1752. PMID: 12524345

23. Houten SM, Wanders RJA. A general introduction to the biochemistry of mitochondrial fatty acid β-oxidation. J Inherited Metab Dis. 2010; 33: 469–477. https://doi.org/10.1007/s10545-010-9061-2 PMID: 20195903

24. Moto K, Yoshiga T, Yamamoto M, Takahashi S, Okano K, Ando T, et al. Pheromone gland-specific fatty-acyl reductase of the silkmoth, *Bombyx mori*. Proc Natl Acad Sci USA. 2003; 100: 9156–9161. https://doi.org/10.1073/pnas.1531993100 PMID: 12871998

25. Chen DS, Dai JQ, Han SC. Identification of the pheromone biosynthesis genes from the sex pheromone gland transcriptome of the diamondback moth, Plutella xylostella. Sci Rep. 2017; 7: 16255. https://doi.org/10.1038/s41598-017-16518-8 PMID: 29176628

26. Zhang YN, Zhang LW, Chen DS, Sun L, Li ZQ, Ye ZF, et al. Molecular identification of differential expression genes associated with sex pheromone biosynthesis in *Spodoptera exigua*. Mol Genet Genomics. 2017; 292: 795–809. https://doi.org/10.1007/s00438-017-1307-3 PMID: 28349297

27. Teal PEA, Tumlinson JH. Properties of cuticular oxidases used for sex pheromone biosynthesis by *Heliothis zea*. J Chem Ecol. 1988; 14: 2131–2145. https://doi.org/10.1007/BF01014254 PMID: 24277148

28. Fang N, Teal PEA, Tumlinson JH. Correlation between glycerolipids and pheromone aldehydes in the sex pheromone gland of female tobacco hornworm moths, Manduca sexta (L.). Arch Insect Biochem Physiol. 1995; 30: 321–336.

29. Bestmann HJ, Herrig M, Attygalle AB. Terminal acetylation in pheromone biosynthesis by Mamestra brassicae L. (Lepidoptera: Noctuidae). Experientia. 1987; 43: 1033–1034.

30. Teal PEA, Tumlinson JH. The role of alcohols in pheromone biosynthesis by two noctuid moths that use acetate pheromone components. Arch Insect Biochem Physiol. 1987; 4: 261–269.

31. Zhu JW, Zhao CH, Lu F, Bengtsson M, Löfstedt C. Reductase specificity and the ratio regulation of E/Z isomers in the pheromone biosynthesis of the European corn borer, Ostrinia nubilalis (Lepidoptera: Pyralidae). Insect Biochem Mol Biol. 1996; 26: 171–176.

32. Gao RT, Qin XX. Preliminary study on Holcocerus insularis. For Pest Dis. 1983: 1, 3–5.

33. Liu HX, Liu ZX, Zheng HX, Jin ZR, Zhang JT, Zhang PQ. Sensilla on the antennae and ovipositor of the carpenterworm, Streltzoviella insularis (Staudinger, 1892) (Lepidoptera, Cossidae). Oriental Insects. 2018; 52: 420–433.

34. Xu LL, Pei JH, Wang T, Ren LL, Zong SX. The larval sensilla on the antennae and mouthparts of five species of Cossidae (Lepidoptera). Can J Zool. 2017; 95: 611–622.

35. Zhang JT, Meng XZ. Electrophysiological responses of Holcocerus insularis Staudinger to the female sex pheromone extracts and standard compounds. Scientia Silvae Sinicae. 2000; 36: 123–126.

36. Zhang JT, Meng XZ. Synthesis and filed tests of sex attractant for Holcocerus insularis Staudinger (Lepidoptera: Cossidae). Scientia Silvae Sinicae. 2001; 37: 71–74.

37. Vogel H, Heidel AJ, Heckel DG, Groot AT. Transcriptome analysis of the sex pheromone gland of the noctuid moth *Heliothis virescens*. BMC Genomics. 2010; 11: 29. https://doi.org/10.1186/1471-2164-11-29 PMID: 20074338

38. Grabherr MG, Haas BJ, Yassour M, Levin JZ, Thompson DA, Amit I, et al. Full-length transcriptome assembly from RNA-Seq data without a reference genome. Nat Biotechnol. 2011; 29: 644–652. https://doi.org/10.1038/nbt.1883 PMID: 21572440

39. Conesa A, Götz S, García-Gómez JM, Terol J, Talón M, Robles M. Blast2GO: A universal tool for annotation, visualization and analysis in functional genomics research. Bioinformatics. 2005; 21: 3674–3676. https://doi.org/10.1093/bioinformatics/bti610 PMID: 16081474

40. Tatusov RL, Koonin EV, Lipman DJ. A genomic perspective on protein families. Science. 1997; 278: 631–637. https://doi.org/10.1126/science.278.5338.631 PMID: 9381173

41. Moriya Y, Itoh M, Okuda S, Yoshizawa AC, Kanehisa M. KAAS: An automatic genome annotation and pathway reconstruction server. Nucleic Acids Res. 2007; 35: W182–W185. https://doi.org/10.1093/nar/gkm321 PMID: 17526522

42. Trapnell C, Williams BA, Pertea G, Mortazavi A, Kwan G, van Baren MJ, et al. Transcript assembly and quantification by RNA-Seq reveals unannotated transcripts and isoform switching during cell differentiation. Nature Biotechnol. 2010; 28: 511–515.

43. Tamura K, Peterson D, Peterson N, Stecher G, Nei M, Kumar S. MEGA5: Molecular evolutionary genetics analysis using maximum likelihood, evolutionary distance, and maximum parsimony methods. Mol Biol Evol. 2011; 28: 2731–2739. https://doi.org/10.1093/molbev/msr121 PMID: 21546353

44. Saitou N, Nei M. The neighbor-joining method: a new method for reconstructing phylogenetic trees. Mol Biol Evol. 1987; 4: 406–425. https://doi.org/10.1093/oxfordjournals.molbev.a040454 PMID: 3447015

45. Rambaut A. FigTree 1.4.2 software. Institute of Evolutionary Biology, Univ. Edinburgh. 2014; Available from: http://tree.bio.ed.ac.uk/software/figtree/

46. Livak KJ, Schmittgen TD. Analysis of relative gene expression data using real-time quantitative PCR and the 2-ΔΔCT method. Methods. 2001; 25: 402–408. https://doi.org/10.1006/meth.2001.1262 PMID: 11846609

47. Raina AK, Jaffe H, Kempe TG, Keim P, Blacher RW, Fales HM, et al. Identification of a neuropeptide hormone that regulates sex pheromone production in female moths. Science. 1989; 244: 796–798. https://doi.org/10.1126/science.244.4906.796 PMID: 17802237

48. Rafaeli A, Bober R, Becker L, Choi MY, Fuerst EJ, Jurenka RA. Spatial distribution and differential expression of the PBAN receptor in tissues of adult Helicoverpa spp. (Lepidoptera: Noctuidae). Insect Mol Biol. 2007; 16: 287–293. https://doi.org/10.1111/j.1365-2583.2007.00725.x PMID: 17328713

49. Jurenka RA, Fabrias G, Roelofs WL. Hormonal control of female sex pheromone biosynthesis in the redbanded leafroller moth, *Argyrotaenia velutinana*. Insect Biochem. 1991; 21: 81–89.

50. Choi MY, Jurenka RA. Role of extracellular Ca2+ and calcium channel activated by a G protein-coupled receptor regulating pheromone production in Helicoverpa zea (Lepidoptera: Noctuidae). Ann Entomol Soc Am. 2006; 99: 905–909.

51. Choi MY, Fuerst EJ, Rafaeli A, Jurenka RA. Identification of a G protein-coupled receptor for pheromone biosynthesis activating neuropeptide from pheromone glands of the moth *Helicoverpa zea*. Proc Natl Acad Sci USA. 2003; 100: 9721–9726. https://doi.org/10.1073/pnas.1632485100 PMID: 12888624

52. Hull JJ, Ohnishi A, Moto K, Kawasaki Y, Kurata R, Suzuki MG, et al. Cloning and characterization of the pheromone biosynthesis activating neuropeptide receptor from the silkmoth, *Bombyx mori*—Significance of the carboxyl terminus in receptor internalization. J Biol Chem. 2004; 279: 51500–51507. https://doi.org/10.1074/jbc.M408142200 PMID: 15358772

53. Kim YJ, Nachman RJ, Aimanova K, Gill S, Adams ME. The pheromone biosynthesis activating neuropeptide (PBAN) receptor of Heliothis virescens: Identification, functional expression, and structure-activity relationships of ligand analogs. Peptides. 2008; 29: 268–275. https://doi.org/10.1016/j.peptides.2007.12.001 PMID: 18243415

54. Lee JM, Hull JJ, Kawai T, Goto C, Kurihara M, Tanokura M, et al. Re-evaluation of the PBAN receptor molecule: characterization of PBANR variants expressed in the pheromone glands of moths. Front Endocrinol. 2012; 3: 6.

55. Hull JJ, Ohnishi A, Matsumoto S. Regulatory mechanisms underlying pheromone biosynthesis activating neuropeptide (PBAN)-induced internalization of the Bombyx mori PBAN receptor. Biochem Biophys Res Commun. 2005; 334: 69–78. https://doi.org/10.1016/j.bbrc.2005.06.050 PMID: 15992769

56. Moore CA, Milano SK, Benovic JL. Regulation of receptor trafficking by GRKs and arrestins. Annu Rev Physiol. 2007; 69: 451–482. https://doi.org/10.1146/annurev.physiol.69.022405.154712 PMID: 17037978

57. Marchese A, Paing MM, Temple BR, Trejo J. G protein—coupled receptor sorting to endosomes and lysosomes. Annu Rev Pharmacol Toxicol. 2008; 48: 601–629. https://doi.org/10.1146/annurev.pharmtox.48.113006.094646 PMID: 17995450

58. Ding BJ, Löfstedt C. Analysis of the *Agrotis segetum* pheromone gland transcriptome in the light of sex pheromone biosynthesis. BMC Genomics. 2015; 16: 711. https://doi.org/10.1186/s12864-015-1909-2 PMID: 26385554

59. Gu SH, Wu KM, Guo YY, Pickett JA, Field LM, Zhou JJ, et al. Identification of genes expressed in the sex pheromone gland of the black cutworm *Agrotis ipsilon* with putative roles in sex pheromone biosynthesis and transport. BMC Genomics. 2013; 14: 636. https://doi.org/10.1186/1471-2164-14-636 PMID: 24053512

60. Nusawardani T, Kroemer JA, Choi MY, Jurenka RA. Identification and characterization of the pyrokinin/pheromone biosynthesis activating neuropeptide family of G protein-coupled receptors from *Ostrinia nubilalis*. Insect Mol Biol. 2013; 22: 331–340. https://doi.org/10.1111/imb.12025 PMID: 23551811

61. Fodor J, Hull JJ, Köblös G, Jacquin-Joly E, Szlanka T, Fónagy A. Identification and functional characterization of the pheromone biosynthesis activating neuropeptide receptor isoforms from *Mamestra brassicae*. Gen Comp Endocrinol. 2018; 258: 60–69. https://doi.org/10.1016/j.ygcen.2017.05.024 PMID: 28579335

62. Golz A, Focke M, Lichtenthaler HK. Inhibitors of *de novo* fatty acid biosynthesis in higher plants. J Plant Physiol. 1994; 143: 426–433.

63. Sasaki Y, Konishi T, Nagano Y. The compartmentation of acetyl-coenzyme A carboxylase in plants. Plant Physiol. 1995; 108: 445–449. https://doi.org/10.1104/pp.108.2.445 PMID: 12228484

64. Harwood JL. Fatty acid metabolism. Annu Rev Plant Physiol Plant Mol Biol. 1988; 39: 101–138.

65. Eliyahu D, Applebaum S, Rafaeli A. Moth sex-pheromone biosynthesis is inhibited by the herbicide diclofop. Pestic Biochem Phys. 2003; 77: 75–81.

66. Tang JD, Charlton RE, Jurenka RA, Wolf WA, Phelan PL, Sreng L, et al. Regulation of pheromone biosynthesis by a brain hormone in two moth species. Proc Natl Acad Sci USA. 1989; 86: 1806–1810. https://doi.org/10.1073/pnas.86.6.1806 PMID: 16594018

67. Jurenka RA, Jacquin E, Roelofs WL. Stimulation of pheromone biosynthesis in the moth *Helicoverpa zea*: Action of a brain hormone on pheromone glands involves $Ca^{2+}$ and cAMP as second messengers. Proc Natl Acad Sci USA. 1991; 88: 8621–8625. https://doi.org/10.1073/pnas.88.19.8621 PMID: 11607216

68. Zhang YN, Xia YH, Zhu JY, Li SY, Dong SL. Putative pathway of sex pheromone biosynthesis and degradation by expression patterns of genes identified from female pheromone gland and adult antenna of Sesamia inferens (Walker). J Chem Ecol. 2014; 40: 439–451. https://doi.org/10.1007/s10886-014-0433-1 PMID: 24817326

69. Hashimoto K, Yoshizawa AC, Okuda S, Kuma K, Goto S, Kanehisa M. The repertoire of desaturases and elongases reveals fatty acid variations in 56 eukaryotic genomes. J Lipid Res. 2008; 49: 183–191. https://doi.org/10.1194/jlr.M700377-JLR200 PMID: 17921532

70. Ikeda Y, Okamura-Ikeda K, Tanaka K. Purification and characterization of short-chain, medium-chain, and long-chain acyl-CoA dehydrogenases from rat liver mitochondria. Isolation of the holo- and apoenzymes and conversion of the apoenzyme to the holoenzyme. J Biol Chem. 1985; 260: 1311–1325. PMID: 3968063

71. Kunau WH, Dommes V, Schulz H. β-Oxidation of fatty acids in mitochondria, peroxisomes, and bacteria: A century of continued progress. Prog Lipid Res. 1995; 34: 267–342. https://doi.org/10.1016/0163-7827(95)00011-9 PMID: 8685242

72. Uchida Y, Izai K, Orii T, Hashimoto T. Novel fatty acid β-oxidation enzymes in rat liver mitochondria. II. Purification and properties of enoyl-coenzyme A (CoA) hydratase/3-hydroxyacyl-CoA dehydrogenase/3-ketoacyl-CoA thiolase trifunctional protein. J Biol Chem. 1992; 267: 1034–1041. PMID: 1730633

73. Sofer W, Martin PF. Analysis of alcohol dehydrogenase gene expression in *Drosophila*. Annu Rev Genet. 1987; 21: 203–227. https://doi.org/10.1146/annurev.ge.21.120187.001223 PMID: 3327463

74. Bohren KM, Bullock B, Wermuth B, Gabbay KH. The aldo-keto reductase superfamily. cDNAs and deduced amino acid sequences of human aldehyde and aldose reductases. J Biol Chem. 1989; 264: 9547–9551. PMID: 2498333

75. Jurenka RA, Roelofs WL. Characterization of the acetyltransferase used in pheromone biosynthesis in moths: specificity for the *Z* isomer in Tortricidae. Insect Biochem. 1989; 19: 639–644.

76. Morse D, Meighen E. Biosynthesis of the acetate ester precursor of the spruce budworm sex pheromone by an acetyl CoA: fatty alcohol acetyltransferase. Insect Biochem. 1987; 17: 53–59.